



HAL
open science

Experimental studies of selected LS-allowed and LS-forbidden transitions of neutral sulfur from the infrared part of the spectrum

A Baclawski, J Musielok

► **To cite this version:**

A Baclawski, J Musielok. Experimental studies of selected LS-allowed and LS-forbidden transitions of neutral sulfur from the infrared part of the spectrum. *Journal of Physics B: Atomic, Molecular and Optical Physics*, 2011, 44 (13), pp.135002. 10.1088/0953-4075/44/13/135002 . hal-00632296

HAL Id: hal-00632296

<https://hal.science/hal-00632296>

Submitted on 14 Oct 2011

HAL is a multi-disciplinary open access archive for the deposit and dissemination of scientific research documents, whether they are published or not. The documents may come from teaching and research institutions in France or abroad, or from public or private research centers.

L'archive ouverte pluridisciplinaire **HAL**, est destinée au dépôt et à la diffusion de documents scientifiques de niveau recherche, publiés ou non, émanant des établissements d'enseignement et de recherche français ou étrangers, des laboratoires publics ou privés.

Experimental studies of selected LS-allowed and LS-forbidden transitions of neutral sulfur from the infrared part of the spectrum

A. Baćłowski and J. Musielok

Institute of Physics, Opole University, ul. Oleska 48, 45-052 Opole, Poland

E-mail: abac@uni.opole.pl and musielok@uni.opole.pl

Abstract. Transition probability ratios ($A_{\text{forb.}}/A_{\text{all.}}$) for eleven line pairs, consisting of one LS-forbidden and one LS-allowed fine structure component of neutral sulfur, are reported. The LS-forbidden transitions belong to two infrared quintet - triplet multiplets: $3d\ ^5D^\circ - 4p\ ^3F$ and $3d\ ^5D^\circ - 4p\ ^3D$. The LS-allowed transitions originate from the same upper terms as the LS-forbidden ones. The A_{ki} ratios are determined by measuring the corresponding line intensity ratios ($I_{\text{forb.}}/I_{\text{all.}}$) from an arc discharge, operated in helium with some admixture of SF_6 . Each selected line pair involves always the same upper energy level and thus the measured line intensity ratio is not affected by non-homogeneities of the plasma source. The transition probability ratios are compared with results of recent advanced calculations.

PACS numbers: 32.30.-r, 32.70.Cs, 32.70.Fw

Submitted to: *J. Phys. B: At. Mol. Phys.*

1. Introduction

Transition probabilities (A_{ki}) of spectral lines are very important quantities for determination of atomic or ionic densities in laboratory plasmas as well as in astrophysical objects. Sulfur is one of the most abundant elements in the universe. Therefore the knowledge of accurate transition probabilities of sulfur spectral lines (line strengths S_{ik} , oscillator strengths f_{ik}) is of great importance for understanding e.g. the formation of stars in their early phase of evolution of the Galaxy, particularly the nucleosynthesis in supernovae [1, 2].

Comprehensive sets of oscillator strengths for neutral sulfur have been recently calculated and published by Zatsarinny and Bartschat [3] as well as by Deb and Hibbert [4], among them also for some infrared intersystem transitions. Zatsarinny and Bartschat [3] applied a modified R-matrix method, based on the B-spline frozen-core representation, while Deb and Hibbert [4] determined oscillator strengths and radiative rates using the Configuration Interaction Version 3 (CIV3) code. In the critical compilation of transition probabilities for sulfur atoms and ions, published recently by the NIST team [5], the data determined by Zatsarinny and Bartschat [3] are recommended in case of S I transitions appearing in the infrared part of the spectrum.

It is well known that calculated oscillator strengths are more reliable for strong transitions than for weaker ones. Therefore it is not surprising that significant disagreements between results of different theoretical approaches are usually observed just for weak transitions, particularly for intersystem lines, because in these cases meaningful cancellations of positive and negative components of the transition integrals occur.

2. Preliminary analysis of theoretical data

In this paper we focused our attention on nine S I intersystem transitions appearing in infrared part of the spectrum. These transitions occur between the lower quintet term $3d\ ^5D^{\circ}$ and two upper triplet terms: $4p\ ^3D$ and $4p\ ^3F$.

Figure 1 shows the partial Grotrian diagram of the S I atomic system. The wavelengths of the S I intersystem transitions (diagonal lines) fall into the spectral range, where also the radiation of two LS-allowed multiplets (vertical lines) come out. Fortunately, the LS-allowed transitions originate from the same upper terms as the studied LS-forbidden lines and involve the lower term $4s\ ^3D^{\circ}$. Therefore, it is an easy task to measure and compare intensity ratios of selected line pairs, consisting of a LS-forbidden and LS-allowed transition and determine in this the corresponding transition probability ratios $A_{\text{forb.}}/A_{\text{all.}}$.

The oscillator strengths for these LS-allowed multiplets, calculated recently by Zatsarinny and Bartschat [3] and Deb and Hibbert [4], are in a reasonable mutual agreement. In the case of the multiplet $4s\ ^3D^{\circ} - 4p\ ^3F$, the largest discrepancy (28%) occurs for the weak transition between the levels $J = 3$ and $J' = 2$. For the other fine

structure components, the differences are in the range from 1% to 9% only. Somewhat worse is the agreement in the case of the $\Delta L = 0$ multiplet $4s' \ ^3D^\circ - 4p' \ ^3D$: the results for the strongest component disagree by about 7%, for all remaining components the data disagree from 1% to 12%. In the case of the above-mentioned intersystem transitions, the discrepancies between these two calculations [3, 4] are significantly larger. In the case of the two strongest components of the multiplet $3d \ ^5D^\circ - 4p' \ ^3F$ (3 - 4 and 2 - 3) the discrepancies are 33% and 15%, while the two weakest components (4 - 3 and 4 - 4) disagree even by factor of 3.8 and 18, respectively. The situation in the case of the multiplet $3d \ ^5D^\circ - 4p' \ ^3D$ is similar, but the discrepancies are somewhat smaller - the stronger components disagree by less than 32%, however the weakest ones (4 - 3 and 0 - 1) differ by factors of 1.5 and 5, respectively. The occurrence of large discrepancies for very weak multiplet components is, to some extent, not surprising - the authors of papers [3, 4] quote for these lines ($\lambda\lambda$ 944.436, 973.0223 and 973.6154 nm) substantially larger uncertainties than for the stronger components.

In table 1, the numerical data on oscillator strengths, for the above-mentioned LS-allowed and LS-forbidden multiplets, taken from literature are listed. The calculations of Refs. [3] and [4] provide not only new f_{ik} values but also the corresponding wavelengths λ_{ki} . The wavelengths obtained by Deb and Hibbert [4] agree satisfactory with experimental values reported by Kaufman and Martin [6], but the wavelengths calculated by Zatsarinny and Bartschat [3] differ from observed by 16 to 21 nm, i.e., about 2% of the wavelength. Since these calculated wavelengths differ somewhat from observed ones, we converted the original oscillator strengths into the corresponding transition probabilities, applying the experimental wavelengths [6] listed in the second column of table 1. For one LS-allowed and five LS-forbidden transitions the wavelengths are not listed in [6], therefore these values we evaluated from the corresponding energy levels quoted in [6]. The A_{ki} values evaluated in this way are also listed in table 1.

The oscillator strengths of Refs. [3] and [4], listed in table 1, are also compared graphically in figure 2, where the ratios $f_{ik}[3]/f_{ik}[4]$ are plotted as functions of $f_{ik}[4]$. As can be seen the discrepancies for LS-forbidden transitions are larger, particularly for weaker transitions.

Oscillator strengths for the LS-forbidden multiplet $3d \ ^5D^\circ - 4p' \ ^3D$ are also reported by Kurucz and Bell [7]. These data are systematically and significantly larger, compared to results of the two above analyzed data sets - the respective f_{ik} ratios are in the range from 2 to 44. Also in case of the LS-allowed multiplet $3d \ ^3D^\circ - 4p' \ ^3D$, the oscillator strength data reported in [7] are systematically larger than those calculated in [3, 4].

Experimental data on S I oscillator strengths (in absolute units) for transitions appearing in the infrared part of the spectrum are reported by Bridges and Wiese [8] (three multiplets) and Zerne et al. [9] (one multiplet). Unfortunately, measurements of the discussed here LS-allowed (as well as LS-forbidden) multiplets have not been performed in these works. In a recent paper, published by one of us (A. B.) [10], relative line strength data within eight infrared LS-allowed multiplets are reported, among them also for the above-mentioned transitions $4s' \ ^3D^\circ - 4p' \ ^3D$ and $4s' \ ^3D^\circ -$

$4p' \ ^3F$. The experimentally determined relative line strengths agree very well with both recent calculations [3, 4]. In the case of the multiplet $4s' \ ^3D^o - 4p' \ ^3D$, the differences do not exceed 5%, with the only exception for the weakest fine structure component that differ by about 40 - 60%. Also in the case of the multiplet $4s' \ ^3D^o - 4p' \ ^3F$, the measured relative line strengths agree with the data of [3] and [4] within uncertainty limits of experiment [10]. Again, only for the weakest fine structure component, the discrepancies are somewhat outside the error limit of our experiment [10]. The agreement between measured relative line strengths and the data resulting from *LS* coupling scheme is only somewhat worse, compared to the agreement with results of Refs. [3] and [4].

3. Excitation source, spectroscopic instrumentation and data acquisition

A wall-stabilized high-current arc, operated at atmospheric pressure, was applied as the excitation source of sulfur atoms. The arc consists of a certain number of water-cooled copper plates, which form a cylindrical discharge channel (4 mm in diameter). Because many details about the arc construction as well as the operating conditions of this plasma source can be found e.g. in our previous papers [11, 12, 13], we present below only some details, which are particular and essential for the present study.

In figure 3 we show the scheme of the central part of the arc construction. Through small gas supply channels in all stabilizing plates (except the very central one), helium was introduced into the cylindrical discharge volume and extracted from it. In the central stabilizing plate a small cylindrical channel was drilled along its radius, serving as input channel for introducing traces of SF_6 gas. The discharge volumes in the vicinity of the two outermost stabilizing plates were fed additionally with some argon, in order to improve the stability of the arc discharge. The small cut (opening) in the insulating spacer, adjacent to the central plate, enabled lateral (side-on) observation of the whole cross section of the plasma column. In this work we operated the arc at a current of 32 ampere, using two different SF_6 gas flows, in order to provide optimal conditions for measuring the arc emission within *S I* spectral transitions (fine structure components) of significantly different intensities. In experiment A, the SF_6 gas flow rate was about 3 times larger than in experiment B, at unchanged working gas flow rates (helium and argon).

In figure 4, the scheme of the optical imaging system is shown. The radiation emitted from the arc in side-on direction, was reflected from the plane and concave mirror ($f = 70$ mm) producing the image of the arc column (magnification 1:1) on the entrance slit of the spectrometer. By turning the plane mirror by 90 degrees, the radiation of the tungsten strip standard source was registered in order to perform spectral calibrations of measured signals from the arc. The measurements were performed applying a grating with 651 grooves/mm. In the exit focal plane of the grating spectrometer a two dimensional optical multichannel analyzer Symphony with 1024×256 pixels (pixel's dimensions: $26 \times 26 \ \mu m$) was mounted. At fixed angular position of the grating, a spectral interval of 19 nm could simultaneously be detected with reciprocal dispersion

of 0.0185 nm/pixel. We set the grating always at angular positions allowing to measure simultaneously intensities of both members of the selected line pairs. In this way our measured line intensity ratios are not affected by possible departures from stability of the arc emission. Other details about the optical imaging and detection system can be found in [10].

The whole detector array was divided in vertical direction into 32 tracks consisting of 8 pixels in that direction. At such division, each track collects the radiation originating from a plasma layer of a height of 0.2 mm. In this way, each exposure of the CCD detector yields 32 spectra, originating from different plasma layers covering the whole arc column. However, for data processing we used always only the 15 spectra originating from the central part of the arc. Figure 3b shows the range of the plasma column that was used for determination of relative S I line intensities. The part of the arc column between the two outermost arrows (along chords), including the central one (along the diameter), was used for determination of S I line intensities. The two outermost plasma volumes along chords (lines of sight) are spaced by 1.5 mm from the arc diameter. The radiation emerging from the arc at both plasma conditions (different SF₆ gas flow rates), was registered several times applying different exposure times. As mentioned in section *Preliminary analysis of theoretical data*, the main challenge of this work is to determine intensity ratios of selected line pairs, consisting of a LS-forbidden and LS-allowed transition. As can be seen from the Grotrian diagram, each LS-forbidden line has at least one "companion" line from among the LS-allowed transitions. Therefore, fortunately the measured line ratios are not affected by possible departures from stability of the arc emission. Similarly, the evident non-homogeneities of the plasma layers along the line of sight do not influence the measured intensity ratios of properly selected line pairs. However, crucial factors for obtaining reliable line intensity ratios are: optically thin conditions of the plasma along the line of sight and the linear response of the detection system. The first factor - the optically thin condition - is facilitated by the short plasma layers and is additionally ensured by adjusting appropriately the SF₆ gas flow rates. The situation is also facilitated by the fact, that the measured lines involve lower levels, which are very far from the S I ground level (more than 8.4 eV) and thus, their populations at our plasma conditions are rather small. The second factor - the linear response of the CCD detector - was carefully checked as described in detail in our recent paper [14].

4. Results and discussion

In figure 5, the arc emission (after radiance calibration) registered at two exposure times of the detector 1.5 and 30 second, are presented. In the upper part of the figure, the spectrum in the wavelength interval 941 - 951 nm is shown. The strong lines in the left hand side of the figure are the LS-allowed lines of the multiplet $4s' \ ^3D^o - 4p' \ ^3F$. The five lines marked with stars belong to the LS-forbidden multiplet $3d \ ^5D^o - 4p' \ ^3F$. At the exposure time of 30 second (lower spectrum), the emission of the strongest LS-allowed

lines caused saturation the CCD detector. Therefore, in the lower spectrum we present only the emission in the wavelength range from 944 to 951 nm. As can be seen, even the weak lines emerge quite well from the continuum background radiation, enabling reliable line intensity measurements to be performed.

In figure 6, the spectra embracing the LS-forbidden and LS-allowed multiplets, originating from the same upper term $4p' \ ^3D$, are presented, again at two different time exposures: 4 and 20 seconds. In both figures (5 and 6), the LS-allowed S I transitions used as reference lines are marked with their corresponding wavelengths and lower-upper J values. Other sulfur lines (also fluorine, argon and nitrogen), which appear in the spectrum, are labeled only with their respective spectroscopic notation.

Detailed analysis of the observed line shapes show that all S I lines exhibit the same profile resulting mainly from instrumental and Doppler broadening. Therefore, all studied line shapes were fitted with identical Voigt profiles, consisting of fixed Gauss and Lorentz components and then integrated, in order to obtain total line intensities. When calculating the line intensity ratios, the very small wavelength dependence of the spectral response of our instrumentation has been taken into account.

In the second column of table 2, the wavelengths of selected line pairs (LS-forbidden / LS-allowed,) in all cases originating from the same upper level are listed. The "individual" line intensity ratios, ($I_{\text{forb.}}/I_{\text{all.}}$), were obtained from each registered spectrum separately. Each registration of the arc emission (exposure of the detector) yields 15 line intensity ratios for each selected line pair. The final determined line intensity ratios are averaged data, obtained from both experiments A and B and from 4 to 8 independent registrations of the arc emission, i.e., from 60 to 120 individual spectra. The averaged line intensity ratios, $I_{\text{forb.}}/I_{\text{all.}}$, were then converted into the corresponding transition probability ratios $A_{\text{forb.}}/A_{\text{all.}}$ according to the formula:

$$\frac{A_{\text{forb.}}}{A_{\text{all.}}} = \frac{\lambda_{\text{forb.}} I_{\text{forb.}}}{\lambda_{\text{all.}} I_{\text{all.}}}, \quad (1)$$

where $\lambda_{\text{forb.}}$ and $\lambda_{\text{all.}}$ are the corresponding wavelengths taken from Ref. [6] (column 2 of table 1).

The experimentally determined transition probability ratios $A_{\text{forb.}}/A_{\text{all.}}$ are listed in column 3 of table 2 and compared with the analogous ratios taken from Refs. [3], [4] and [7]. The error limits quoted in table 2, include contributions from:

- the doubled standard deviation for each individual ratio (typically from 0.4 to 2.6 %, with exception of the line pairs number 6 and 7, where it does not exceed 6%),
- the possible small error originating from radiance calibration (less than 1%, since the wavelength differences are very small),
- the line shape fitting procedure - typically from 3 to 5%, with exception of three LS-forbidden lines at wavelengths 947.983, 950.121 and 969.1604 nm, being weak or situated at the wings of significantly stronger components, where the fitting error

is about 20% (for the first two mentioned lines) and may reach even 50% for the last transition,

- possible departure from optically thin conditions of the plasma layers (1%) and
- possible departure from linearity of the response of the detection system (1%).

As can be seen, the largest contribution to the uncertainty of our measurements arises from the line fitting procedure. However, by keeping the widths of the Voigt profile fixed, this possible error source has been minimized. This contribution is obviously significantly larger, when the studied ratio involves a very weak line. In case of line pairs, with similar and not too small intensities, these uncertainties do not exceed 4%. The final uncertainties, quoted in table 2, are square roots of the sums of all squared error sources.

The experimentally determined transition probability ratios are also compared in figure 7 with results of calculations [3] and [4], where the ratios $\{(A_{\text{forb.}}/A_{\text{all.}})^{\text{calc.}}/(A_{\text{forb.}}/A_{\text{all.}})^{\text{expt.}}\}$ are shown versus the product $g_k A_{ki}$ for the LS-forbidden line. The statistical weight (g_k) is equal to $2J_k+1$, where J_k is the total momentum quantum number of the upper level of the considered transition. The A_{ki} values have been taken from Deb and Hibbert [4]. The marked error bars result exclusively from uncertainties of our experiment. On average, the experimental data show better agreement with calculations of Deb and Hibbert [4]: eight A_{ki} ratios (out of eleven) are within the error limits of our measurements (for comparison, when the data of Zatsarinny and Bartschat [3] are used, only four ratios agree within these limits). Only in the case of two studied ratios, #4 and #8, the measured results depart significantly from data resulting from both recent calculations, which are in rather good mutual agreement.

In the case of ratio #4, the measured value is about factor of 1.3 and 1.5 larger than the result based on data of Refs. [3] and [4], respectively. The LS-allowed transition involved in this ratio (944.503 nm) has been, among others transitions, studied in the recent experimental paper by Baćlawski [10]. Unfortunately, this paper provides only relative transition probabilities within given multiplets. However, the relative line strengths measured for the multiplet $4s' \ ^3D^{\circ} - 4p' \ ^3F$ show very good agreement with results of calculations [3] and [4], except just the result for the line at 944.503 nm. The obtained ratios $A_{\text{calc.}}/A_{\text{expt.}}$ for this line are: 1.13 and 1.24, for Refs. [3] and [4] respectively. If we correct the theoretical A_{ki} data (decrease their values by factors 1.13 and 1.24), the ratios $A_{\text{forb.}}/A_{\text{all.}}$ listed in column 5 and 6 of table 2, will amount to 0.26 (for both calculations) and will be considerably closer to the measured ratio (0.31 ± 0.02).

Similar situation is found in the case of the studied ratio # 8: the measured ratio $(A_{\text{forb.}}/A_{\text{all.}})^{\text{expt.}}$ is greater by factors 2 and 1.7 than the ratios based on data of Refs. [3] and [4]. The LS-allowed transition at 963.313 nm, used as reference line, belongs to the multiplet $4s' \ ^3D^{\circ} - 4p' \ ^3D$. This transition is the only one (within this multiplet) where large discrepancies between measured [10] and calculated data [3, 4] are encountered.

The experimentally determined (relative) line strength is greater by factors 1.44 and 1.58 than the corresponding calculated ones. Similar A_{ki} corrections as for the previous case lead to $A_{\text{forb.}}/A_{\text{all.}}$ ratios of 4.9 and 6.3, which are significantly closer to the experimental ratio 6.9 ± 0.3 .

5. Conclusions

Our analysis of measured line intensity ratios and comparison with results of recent advanced calculations of oscillator strengths for the S I spectrum [3, 4] lead us to three main conclusions: (i) both recent calculations yield, generally speaking, quite good atomic structure data (oscillator strengths) even for weaker lines, including intersystem transitions (except very weak transitions with $f_{ik} < 10^{-4}$); (ii) the CIV3 calculations by Deb and Hibbert [4] provide somewhat more reliable data than those reported by Zatsarinny and Bartschat [3]; (iii) some encountered discrepancies between measured and calculated transition probability ratios confirm recent measurements [10], where in case of some infrared multiplets, weak fine structure components were found to be somewhat weaker than expected from LS coupling scheme as well as from recent calculated data.

References

- [1] Nakamura T, Umeda H, Iwamoto K, Nomoto K, Hashimoto M, Hix W R and Thielemann F-K 2001 *Astrophys. J.* **555** 880–99
- [2] Takeda Y, Hashimoto O, Taguchi H, Yoshioka K, Takada-Hidai M, Saito Y and Honda S 2005 *Publ. Astron. Soc. Japan* **57** 751–68
- [3] Zatsarinny O and Bartschat K 2006 *J. Phys. B: At. Mol. Opt. Phys.* **39** 2861–75
- [4] Deb N C and Hibbert A 2008 *At. Data Nucl. Data Tables* **94** 561–602
- [5] Podobedova L I and Kelleher D E 2009 *J. Phys. Chem. Ref. Data* **38** 171–439
- [6] Kaufman V and Martin W C 1993 *J. Phys. Chem. Ref. Data* **22** 279–375
- [7] Kurucz R L and Bell B 1995 *Atomic Line Data Kurucz CD-ROM No. 23* (Cambridge, Mass.: Smithsonian Astrophysical Observatory)
- [8] Bridges J M and Wiese W L 1967 *Phys. Rev.* **159** 31–8
- [9] Zerne R, Caiyan L, Berzinsh U and Svanberg S 1997 *Phys. Scr.* **56** 459–61
- [10] Baclawski A 2011 *Europ. Phys. J. D* **61** 327–34
- [11] Wujec T, Baclawski A, Goly A and Książek I 1999 *Acta Phys. Polon. A* **96** 333–40
- [12] Książek I and Musielok J 2000 *Contrib. Plasma Phys.* **40** 141–6
- [13] Wujec T, Olchawa W, Halenka J and Musielok J 2002 *Phys. Rev. E* **66** 066403
- [14] Baclawski A and Musielok J 2008 *Spectrochim. Acta* **63** 1315–9

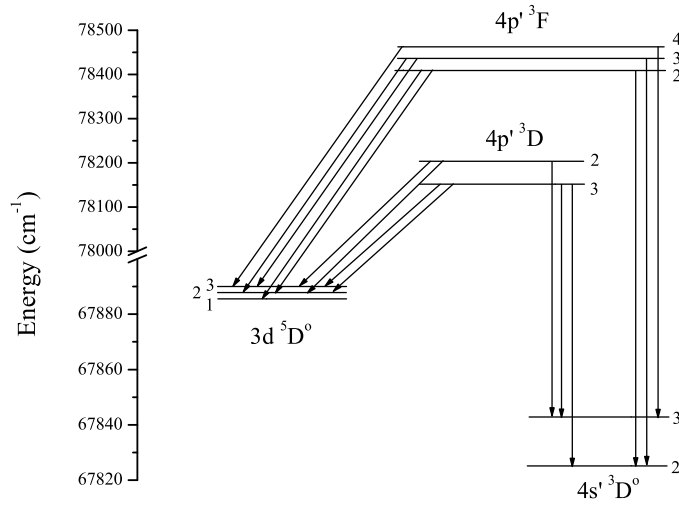


Figure 1. The partial Grotrian diagram of the sulfur atom (S I) is shown. The diagonal lines correspond to intersystem transitions studied in this work. The vertical lines represent S I LS-allowed transitions, used as reference transitions.

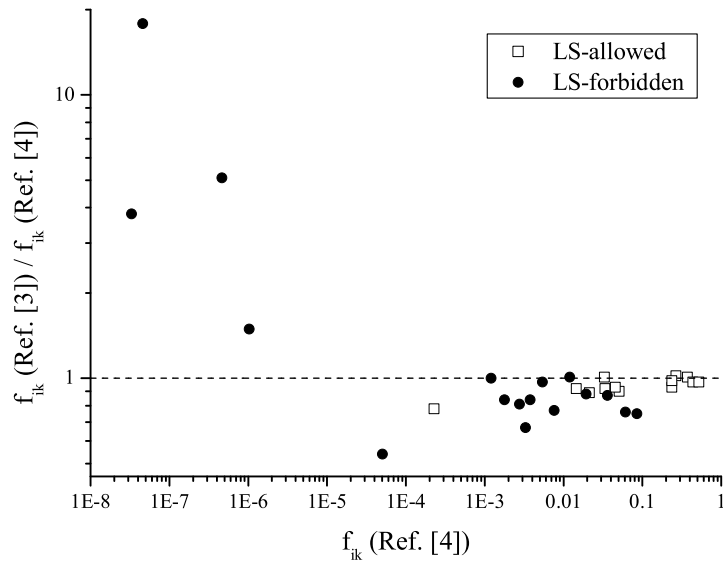


Figure 2. Theoretically determined oscillator strength data for two LS-forbidden and two LS-allowed S I multiplets, taken from Refs. [3] and [4], are compared. The ratios $f_{ik}[3]/f_{ik}[4]$ are shown as function of f_{ik} values reported in [4]. In case of LS-allowed multiplets the agreement is good, with exception of the weakest fine structure component $4s' \ ^3D_3^0 - 4p' \ ^3F_2$. For majority of LS-forbidden transitions the calculations disagree substantially: for stronger lines the f_{ik} data of Ref. [3] are smaller, while for the weaker ones they are significantly larger than those of Ref. [4].

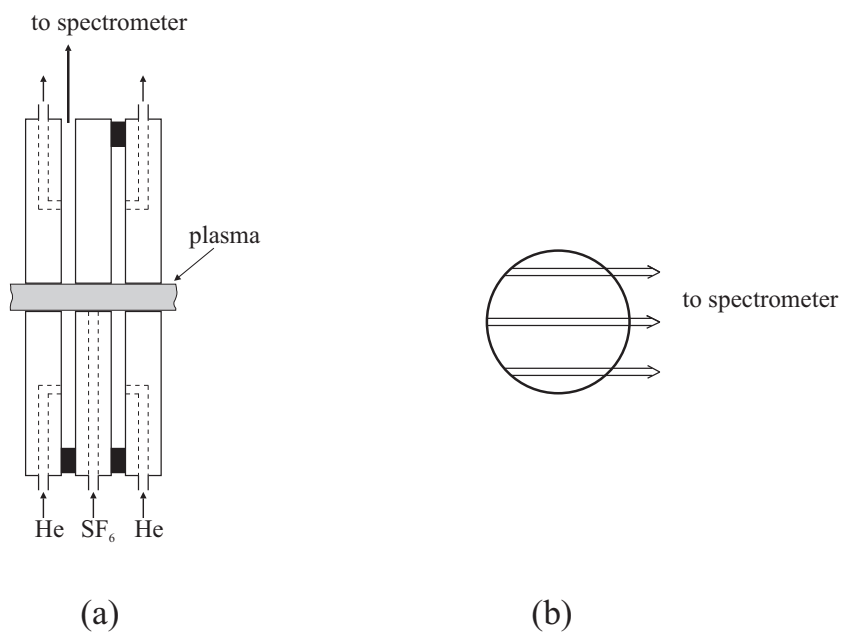


Figure 3. Shown are: (a) - the scheme of the central part of the arc construction, and (b) - the part of the arc column used for studying the S I emission emerging in side on direction (for details see the text below).

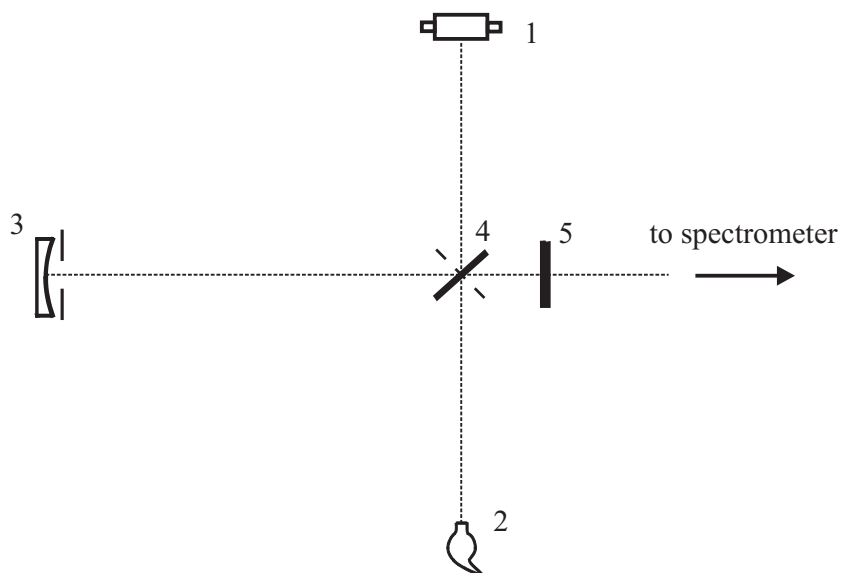


Figure 4. The optical imaging system of the spectroscopic setup is shown. The numbers 1 and 2 denote the arc (excitation source) and the radiation standard source (tungsten strip lamp), 3 and 4 stand for concave and plane mirror, and 5 denotes the spectral filter blocking the radiation originating from higher order spectra. The small plane mirror (4) is placed slightly below the optical axis of the spectrometer.

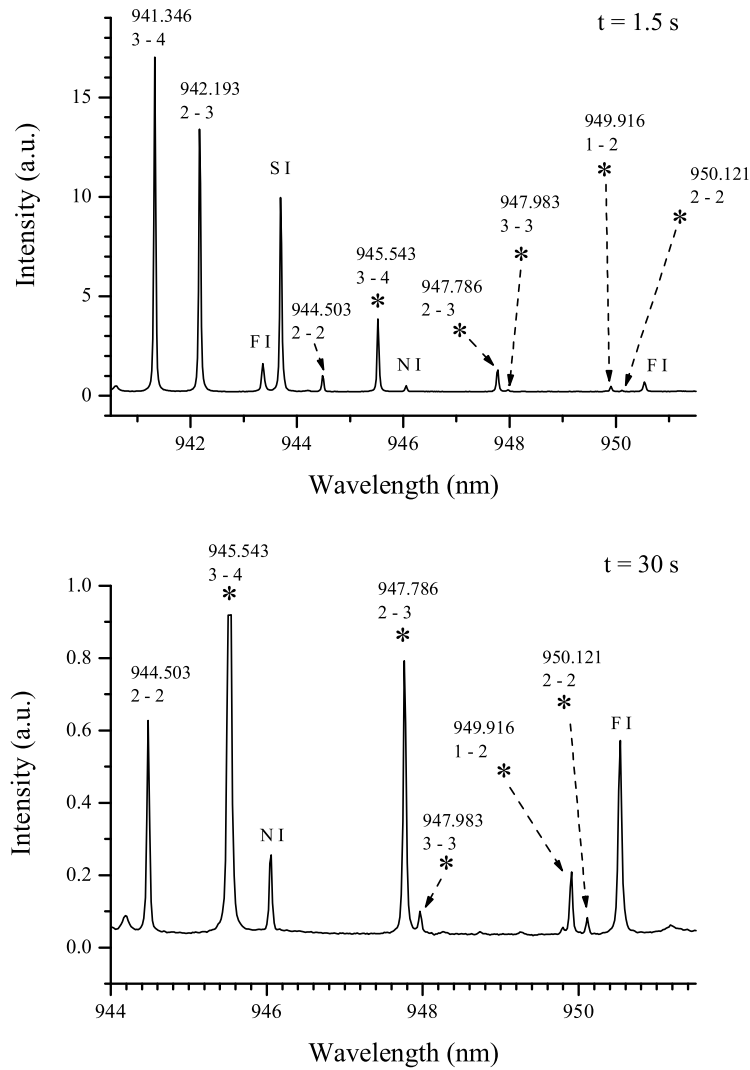


Figure 5. Arc spectra, taken at two exposure times of the detector, are shown. In the upper part of the figure (exposure time 1.5 s), the wavelength interval 941 - 951 nm is shown, where five LS-allowed and five LS-forbidden fine structure components of the multiplets $4s' \ ^3D^\circ - 4p' \ ^3F$ and $3d \ ^5D^\circ - 4p' \ ^3F$ appear. The LS-forbidden transitions are marked with stars and their respective lower - upper J values. The LS-allowed transitions, applied as reference lines, are also marked with the corresponding J -values. In the lower part of the figure, only a section of the spectrum, taken at significantly larger exposure time, is presented. As can be seen, the weak lines emerge quite well from the continuum background radiation, enabling reliable line intensity measurements to be performed. The sulfur line at 943.7 nm (marked with S I) consists of two overlapping fine structure components, originating from two different upper levels, and therefore this line could not be applied as reference line.

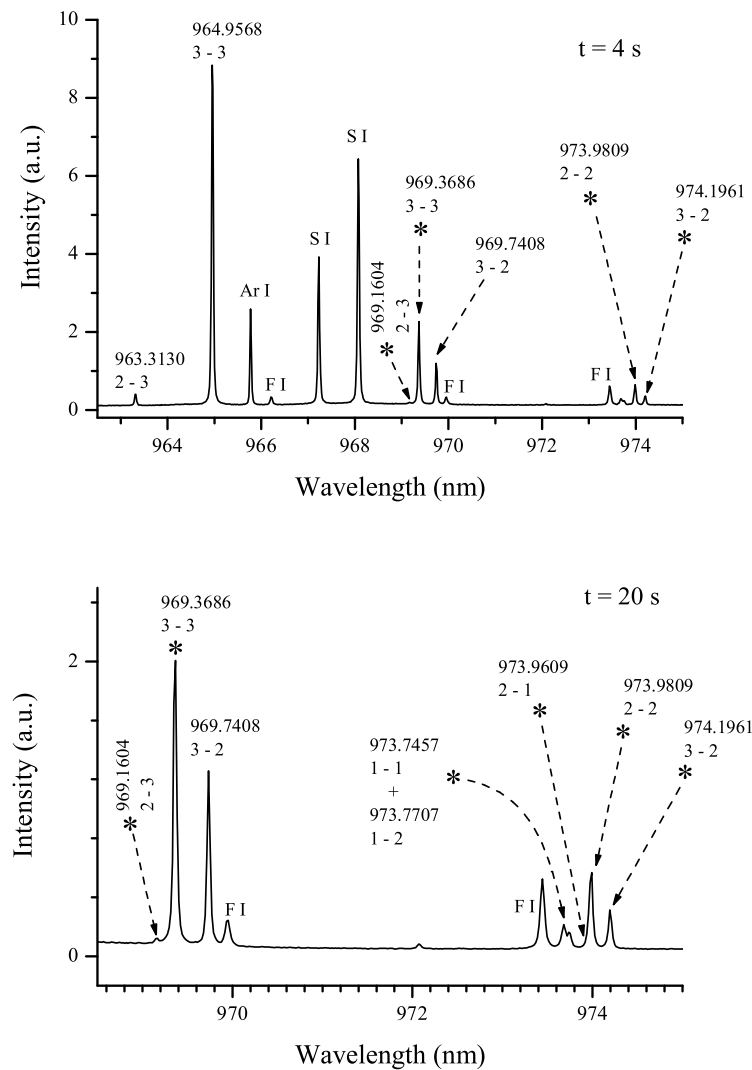


Figure 6. The arc spectra in the wavelength range 963 - 975 nm (upper part, exposure time 4 s) and 969.3 - 974.5 nm (lower part, exposure time 20 s) are shown. The LS-forbidden transitions are marked with stars and their respective lower - upper J values. The LS-allowed transitions, applied as reference lines, are also marked with the corresponding J -values. From among the six marked LS-forbidden transitions, only for four of them at wavelengths 969.16, 969.37, 973.98 and 974.19 nm, intensity measurements with reasonable uncertainty could be performed. On the blue wing of the line at 973.98 a much weaker line at 973.96 appears, which - according to calculations [3, 4] - is about one order of magnitude weaker.

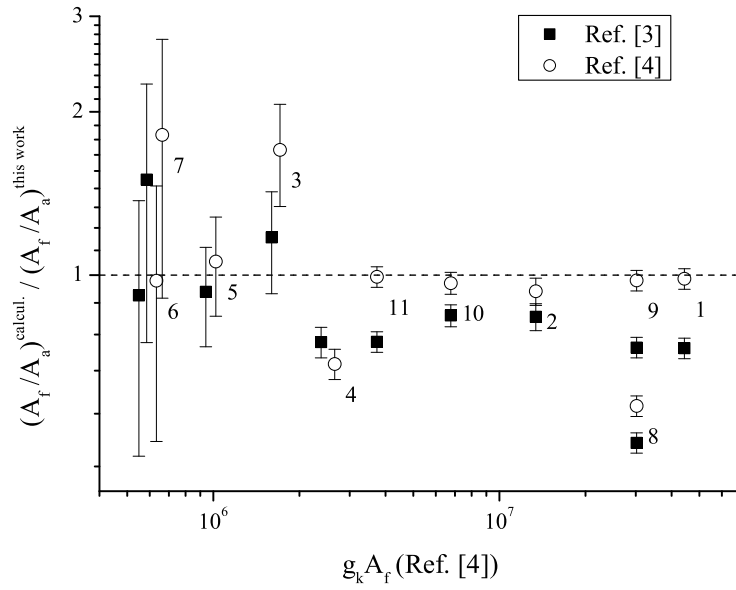


Figure 7. The quotients of transition probability ratios (calculated to measured data) are shown versus the product $g_k A_{ki}$ for the *LS*-forbidden line. The statistical weight (g_k) is equal to $2J_k+1$, where J_k is the total momentum quantum number of the upper level of the considered transition. The A_{ki} values have been taken from Deb and Hibbert [4]. The error bars result exclusively from uncertainties of our experiment. The numbers nearby the symbols refer to pair numbers in column 1 of table 2. For transparency of the figure, the data related to pairs # 3 - 7 are slightly shifted on the abscissa of the graph.

Tables and table captions

Table 1. Recently published theoretical oscillator strengths and transition probabilities for two LS-allowed and two LS-forbidden multiplets of neutral sulfur (S I) are compared.

Transition	λ (nm)	f_{ik}			A_{ki} (s^{-1})			
		Ref. [6]	Ref. [3]	Ref. [4]	Ref. [7]	Ref. [3]	Ref. [4]	Ref. [7]
LS-allowed $4s' - 4p'$								
$^3D_3^o - ^3F_4$	941.346		3.77E-01	3.73E-01		2.21E+07	2.18E+07	
$^3D_2^o - ^3F_3$	942.193		4.26E-01	4.37E-01		2.29E+07	2.35E+07	
$^3D_1^o - ^3F_2$	943.711		5.02E-01	5.19E-01		2.26E+07	2.33E+07	
$^3D_3^o - ^3F_3$	943.760		1.34E-02	1.45E-02		1.00E+06	1.09E+06	
$^3D_2^o - ^3F_2$	944.503		3.07E-02	3.35E-02		2.30E+06	2.50E+06	
$^3D_3^o - ^3F_2$	946.079*		1.77E-04	2.27E-04		1.85E+04	2.37E+04	
$^3D_2^o - ^3D_3$	963.3130	1.90E-02	2.13E-02	5.64E-02	9.75E+05	1.09E+06	2.89E+06	
$^3D_3^o - ^3D_3$	964.9568	2.72E-01	2.67E-01	3.20E-01	1.95E+07	1.92E+07	2.29E+07	
$^3D_1^o - ^3D_1$	967.2283	2.20E-01	2.36E-01	2.71E-01	1.57E+07	1.68E+07	1.93E+07	
$^3D_1^o - ^3D_2$	967.2531	4.57E-02	5.06E-02	8.97E-02	1.95E+06	2.17E+06	3.84E+06	
$^3D_2^o - ^3D_1$	968.0561	4.23E-02	4.54E-02	5.38E-02	5.02E+06	5.39E+06	6.38E+06	
$^3D_2^o - ^3D_2$	968.0809	2.31E-01	2.36E-01	2.52E-01	1.64E+07	1.68E+07	1.79E+07	
$^3D_3^o - ^3D_2$	969.7408	3.33E-02	3.29E-02	4.03E-02	3.31E+06	3.27E+06	4.00E+06	
LS-forbidden $3d - 4p'$								
$^5D_3^o - ^3F_4$	945.543		6.42E-02	8.51E-02		3.73E+06	4.94E+06	
$^5D_2^o - ^3F_3$	947.786		3.14E-02	3.60E-02		1.67E+06	1.91E+06	
$^5D_3^o - ^3F_3$	947.983		2.21E-03	3.29E-03		1.64E+05	2.44E+05	
$^5D_1^o - ^3F_2$	949.916		1.21E-02	1.20E-02		5.37E+05	5.32E+05	
$^5D_2^o - ^3F_2$	950.121		2.23E-03	2.76E-03		1.65E+05	2.04E+05	
$^5D_4^o - ^3F_4$	944.436*		8.16E-07	4.57E-08		6.10E+01	3.42E+00	
$^5D_3^o - ^3F_2$	950.319*		2.75E-05	5.05E-05		2.84E+03	5.22E+03	
$^5D_4^o - ^3F_3$	946.872*		1.26E-07	3.32E-08		1.21E+01	3.17E+00	
$^5D_2^o - ^3D_3$	969.1604	1.50E-03	1.78E-03	5.02E-02	7.61E+04	9.05E+04	2.55E+06	
$^5D_3^o - ^3D_3$	969.3686	4.65E-02	6.08E-02	1.13E-01	3.30E+06	4.32E+06	8.05E+06	
$^5D_1^o - ^3D_1$	973.7457	5.25E-03	5.39E-03	8.37E-02	3.69E+05	3.79E+05	5.89E+06	
$^5D_1^o - ^3D_2$	973.7707	1.20E-03	1.20E-03	5.28E-02	5.06E+04	5.09E+04	2.23E+06	
$^5D_2^o - ^3D_1$	973.9609	3.16E-03	3.75E-03	5.02E-02	3.70E+05	4.39E+05	5.88E+06	
$^5D_2^o - ^3D_2$	973.9859	1.70E-02	1.93E-02	1.00E-01	1.20E+06	1.36E+06	7.04E+06	
$^5D_3^o - ^3D_2$	974.1961	5.83E-03	7.59E-03	4.52E-02	5.74E+05	7.47E+05	4.44E+06	
$^5D_4^o - ^3D_3$	973.0223*	1.53E-06	1.03E-06		1.39E+02	9.29E+01		
$^5D_0^o - ^3D_1$	973.6154*	2.36E-06	4.63E-07		5.54E+01	1.09E+01		

* lines not listed in [6], the wavelengths have been calculated from energy levels contained therein.

Table 2. The experimentally determined transition probability ratios $A_{\text{forb.}}/A_{\text{all.}}$ are compared with results of calculations.

Pair No	$\lambda_{\text{forb.}}/\lambda_{\text{all.}}$	$A_{\text{forb.}}/A_{\text{all.}}$			
		This work	Ref. [3]	Ref. [4]	Ref. [7]
1	945.543 / 941.346	0.23 ± 0.01	0.169	0.227	
2	947.786 / 942.193	0.087 ± 0.005	0.0729	0.0813	
3	947.983 / 942.193	0.0061 ± 0.0013	0.00716	0.0104	
4	949.916 / 944.503	0.31 ± 0.02	0.233	0.213	
5	950.121 / 944.503	0.077 ± 0.016	0.0717	0.0816	
6	969.1604 / 963.3130	0.085 ± 0.042	0.0781	0.0830	0.881
7	969.1604 / 964.9568	0.0026 ± 0.0013	0.00390	0.00471	0.111
8	969.3686 / 963.3130	6.9 ± 0.3	3.38	3.96	2.78
9	969.3686 / 964.9568	0.23 ± 0.01	0.169	0.225	0.352
10	973.9869 / 969.7408	0.43 ± 0.02	0.363	0.416	1.76
11	974.1961 / 969.7408	0.23 ± 0.01	0.173	0.228	1.11